Nuclear magnetic dipole moment of ^{209}Bi from NMR experiments

Andrej Antušek*
Slovak University of Technology in Bratislava, ATRI, Faculty of Materials Science and Technology in Trnava, J. Bottu 25, 917 24 Trnava, Slovak Republic

Michal Repisky
Hylleraas Centre for Quantum Molecular Sciences, Department of Chemistry, UiT – The Arctic University of Norway, N-9037 Tromsø, Norway

Michał Jaszuński
Institute of Organic Chemistry, Polish Academy of Sciences, Kasprzaka 44, 01-224 Warsaw, Poland

Karol Jackowski, Włodzimierz Makulski, and Maria Misiak
Laboratory of NMR Spectroscopy, Department of Chemistry, University of Warsaw, Pasteura 1, 02-093 Warsaw, Poland

(Received 28 June 2018; published 19 November 2018)

We report the ^{209}Bi magnetic moment derived from NMR experiments and first-principles calculated shielding constants of Bi^{3+} ions in aqueous solutions of $Bi(NO_3)_3$ and $Bi(ClO_4)_3$ salts. Our values represent an independent confirmation of the ^{209}Bi magnetic moment recently determined by Skripnikov *et al.* [L. V. Skripnikov *et al.*, Phys. Rev. Lett. **120**, 093001 (2018)], which is of utmost importance for the interpretation of Bi^{82+} ion hyperfine splitting experiments. The accuracy limit of the ^{209}Bi magnetic moment set by the present computational chemistry methods is discussed.

DOI: 10.1103/PhysRevA.98.052509

I. INTRODUCTION

The nuclear magnetic dipole moment of ^{209}Bi, $\mu_I(^{209}\mathrm{Bi})$, belongs to the largest magnetic moments of the stable and long-lived nuclei [1]. This fact together with the high electric charge of the bismuth nucleus implies that an electron in a hydrogenlike Bi^{82+} ion experiences the strongest magnetic field achievable in the laboratory. The hyperfine splitting (HFS) as a sensitive probe of electron-nucleus interactions became for more than two decades a test of quantum electrodynamics (QED) effects in Bi^{82+} [2–5]. The discrepancy between measurements and the theoretical prediction of Bi^{82+} HFS raised the question of strong-field modifications of QED. However, because the HFS is proportional to the nuclear magnetic moment, the error in the ^{209}Bi nuclear magnetic moment measurement was identified as a possible origin of HFS discrepancy and a remeasurement of the nuclear magnetic dipole moment of ^{209}Bi was requested [6].

Numerous tabulated values of nuclear magnetic moments are derived from nuclear magnetic resonance (NMR) experiments [1]. These values, mostly measured in the 1960s and 1970s, are influenced by a systematic error due to the inaccurate description of the NMR shielding needed for their derivation [7]. The development of accurate quantum chemistry methods for the calculation of the shielding constants [8–15] brought the possibility to correct these moments [7]; the corrected nuclear magnetic dipole moments based on gas-phase NMR experiments and state-of-the-art calculations were reported in several reviews and book chapters [16–18]. Another set of corrected nuclear magnetic moments is based on recent calculations of NMR shielding of aqueous cations [19–22]. Both approaches—gas-phase NMR and aqueous cation NMR—were recently applied to ^{207}Pb, providing consistent values for its nuclear magnetic moment [23].

A recent measurement of ^{209}Bi nuclear magnetic moment [5] and a recent hyperfine splitting experiment on bismuth [3] (see also Ref. [4]) brought the experimental and theoretical data for the Bi^{82+} hyperfine splitting into agreement, resolving the longstanding bismuth hyperfine puzzle. This value of $\mu_I(^{209}\mathrm{Bi})$ determined by Skripnikov *et al.* [5] is based on a recent NMR experiment for the BiF_6^- anion in acetonitrile solvent and first-principles calculations of NMR shielding of bismuth in the isolated BiF_6^- anion.

In this work, we present the magnetic moment of ^{209}Bi derived from our experimental data for two different aqueous solutions of Bi^{3+} cations and corresponding first-principles calculations. We demonstrate the robustness of the calculations of NMR shielding for solvated heavy cations and show that standard computational chemistry methods for the shielding and nuclear magnetic dipole moments yield results consistent with Ref. [5]. Our present results provide an independent confirmation of the magnetic moment value of ^{209}Bi given by Skripnikov *et al.* [5].

II. NMR EXPERIMENT

The NMR resonance frequency of ^{209}Bi was measured in aqueous solutions of bismuth(III) nitrate [$Bi(NO_3)_3$] and

*andrej.antusek@stuba.sk

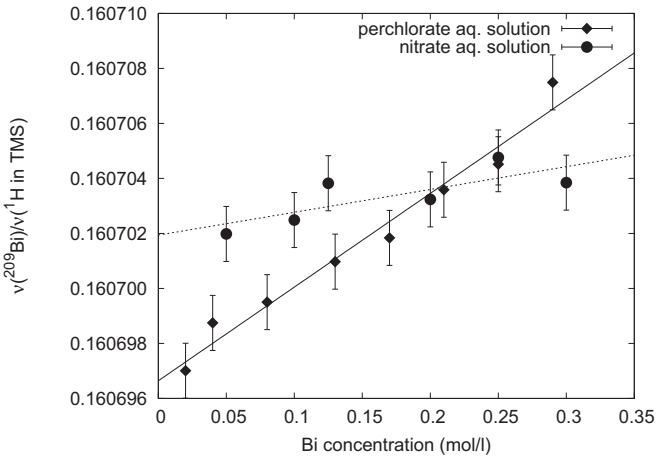

FIG. 1. Concentration dependence of $\nu(^{209}\mathrm{Bi})/\nu(^{1}\mathrm{H}$ in TMS) resonance frequency ratio for $Bi(NO_3)_3$ and $Bi(ClO_4)_3$ in aqueous solutions, respectively. ^{1}H NMR frequency was measured for pure liquid TMS.

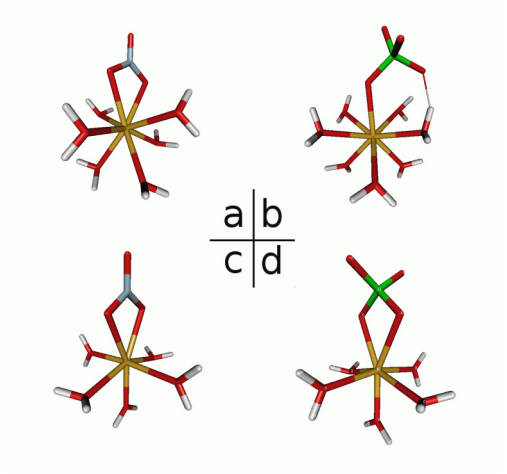

FIG. 2. Stick representation of the structure of aqueous complexes with nitrate and perchlorate anions (symmetry point group in brackets): (a) $(Bi(H_2O)_6NO_3)^{2+}$ [C_1], (b) $(Bi(H_2O)_7ClO_4)^{2+}$ [C_1], (c) $(Bi(H_2O)_5NO_3)^{2+}$ [C_{2v}], (d) $(Bi(H_2O)_5ClO_4)^{2+}$ [C_{2v}]. Color code: hydrogen white, nitrogen blue, oxygen red, chlorine green, bismuth yellow.

bismuth(III) perchlorate [$Bi(ClO_4)_3$]. The preparation of solutions is hindered by the low solubility of bismuth salts in water and various effects such as hydrolysis [24] and the creation of oxyclusters of bismuth [25]. These adverse effects are suppressed in acidic solutions giving, at the same time, an increase in Bi^{3+} solubility. The bismuth salt solution preparation is described in Appendix A.

^{209}Bi NMR experiments were conducted at 300 K on a Varian INOVA-500 spectrometer equipped with a two-channel Varian sw5 probe operating at 80.4 MHz for the bismuth frequency. The ^{209}Bi spectra were recorded with 25 600 scans, pulse width 80 μs (90° pulse), 100 kHz spectral width, acquisition time of 0.05 s, and a relaxation delay of 0.1 s. An exponential function with line broadening of 100 Hz was applied prior to Fourier transformation. The sample of $Bi(NO_3)_3$ in concentrated nitric acid (HNO_3) was used as the external reference standard. Bulk susceptibility effects were not considered.

NMR resonance frequencies of ^{209}Bi were measured in a wide range of bismuth cation concentrations in nitrate and perchlorate acid aqueous solutions. The concentration dependence of the frequency ratio with respect to the ^{1}H NMR frequency in liquid tetramethylsilane (TMS), $\nu(^{1}\mathrm{H}\ \mathrm{in\ TMS}) = 500\,606\,120$ Hz, is shown in Fig. 1. The ^{209}Bi NMR frequency extrapolated to the infinitely dilute solution is 80 445 750.7 Hz and 80 448 374.6 Hz for perchlorate and nitrate, respectively. The chemical shift of Bi^{3+} in aqueous $Bi(ClO_4)_3$ with respect to Bi^{3+} in aqueous $Bi(NO_3)_3$ is -32 ppm [Bi^{3+} in aqueous $Bi(ClO_4)_3$ solution is more shielded than Bi^{3+} in aqueous $Bi(NO_3)_3$].

III. NMR SHIELDING CALCULATIONS

The structure of the Bi^{3+} solvation shell for $Bi(ClO_4)_3$ in aqueous solution is known from extended x-ray absorption fine-structure (EXAFS) and large-angle x-ray scattering (LAXS) experiments [26]. The actual structure depends on the concentration; for higher concentrations, two perchlorate anions take part in the first solvation shell of Bi^{3+}, and for lower concentrations, the number of perchlorate anions in the first solvation shell of Bi^{3+} is reduced to one. The bismuth-oxygen coordination number remains to be eight for a wide range of concentrations [26]. We did not find analogous structural experimental data for aqueous solutions of $Bi(NO_3)_3$ but, in accordance with perchlorate experiments, we assume that for low concentrations, one nitrate anion coordinates with Bi^{3+} together with water molecules in the first solvation shell. The structures of the aqueous complexes $(Bi(H_2O)_6NO_3)^{2+}$ and $(Bi(H_2O)_7ClO_4)^{2+}$, which correspond to experimental conditions in nitrate and perchlorate environments, were optimized using theoretical methods. In addition, the complexes $(Bi(H_2O)_5NO_3)^{2+}$ and $(Bi(H_2O)_5ClO_4)^{2+}$ with C_{2v} space-group symmetry were optimized for benchmark coupled-cluster calculations. The structure of the complexes is depicted in Fig. 2. See, also, Appendix B for methods and optimization procedure details.

The shielding constants $\sigma(^{209}\mathrm{Bi})$ in the aqueous complexes were calculated applying both nonrelativistic and relativistic approaches. For nonrelativistic NMR shielding calculations, we applied the Hartree-Fock (HF) method, a sequence of correlation methods including second-order perturbation theory (MP2) [8], coupled cluster with single and double excitations (CCSD) [10], and coupled-cluster method with noniterative incorporation of triple excitations [CCSD(T)] [9], as well as density functional theory (DFT) method with the Perdew-Burke-Ernzerhof (PBE0) functional [27,28]. We used the uncontracted ANO-RCC [29] basis set for bismuth combined with the cc-pVDZ [30] basis set for hydrogen, nitrogen, oxygen, fluorine, and chlorine atoms (this basis-set combination is called uANO.dz). In all nonrelativistic methods, gauge-including atomic orbitals (GIAOs) [31] were applied to ensure gauge-origin independence of the computed shielding constants. Nonrelativistic correlated calculations were carried out with the CFOUR package [32]; nonrelativistic PBE0 shielding constants were obtained using the NWChem

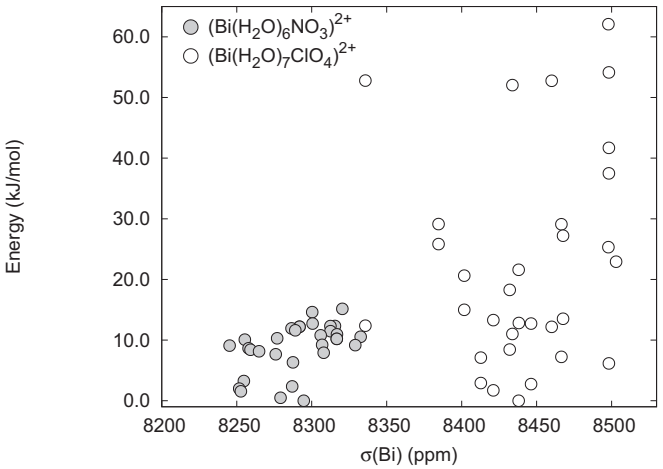

FIG. 3. Nonrelativistic Hartree-Fock NMR shielding of bismuth vs energy of $(Bi(H_2O)_7ClO_4)^{2+}$ and $(Bi(H_2O)_6NO_3)^{2+}$ complexes calculated for various local minimum structures optimized at the DFT level. For both data sets, the energy is plotted relative to the structure with the lowest energy (see Appendix B for details).

package [33]. Relativistic shielding constants were calculated at two levels of theory: Dirac-Hartree-Fock (DHF) and Dirac-Kohn-Sham (DKS) with the PBE0 functional. For relativistic calculations, we have used the uncontracted ANO-RCC basis set for bismuth combined with uncontracted cc-pVDZ [30] for other elements (uANO.udz). To examine the basis-set convergence, Dyall's vDZ, vTZ, and vQZ series was used [34]. GIAOs were used in all relativistic calculations. The small-component basis set was generated employing the restricted magnetic balance scheme [35,36]. In the relativistic shielding calculations, nuclei were represented by a Gaussian charge distribution [37]. All relativistic calculations were carried out using the ReSpect package [38].

First, $\sigma(^{209}\mathrm{Bi})$ was calculated at the Hartree-Fock level of theory for all identified stable conformers of the hydrated Bi^{3+} complexes. Despite large differences in the energies of these structures, the shielding of bismuth lies in a narrow interval of 100 and 200 ppm for the $(Bi(H_2O)_6NO_3)^{2+}$ and $(Bi(H_2O)_7ClO_4)^{2+}$ structures, respectively. The NMR shielding vs energy plot (Fig. 3) illustrates the structural robustness of the solvated cation approach for the prediction of the shielding. The shielding of the central Bi^{3+} cation shows low sensitivity to the actual structure of the solvation shell—a feature which we have also observed in our previous cation studies [19–22]. Although the Bi chemical shift between the lowest-energy structures of $(Bi(H_2O)_6NO_3)^{2+}$ and $(Bi(H_2O)_7ClO_4)^{2+}$ (−150 ppm) is somewhat larger than experimentally determined (−32 ppm), in agreement with experiment Bi^{3+} in a perchlorate solution is more shielded than in a nitrate solution in our model solvation structures. We note that most structures represented in Fig. 3 are inaccessible at 300 K; the energy differences with respect to the lowest-energy structures correspond to $\approx 10^3$ Kelvin.

To obtain accurate shielding constants for compounds containing heavy elements, both electron correlation and relativity have to be properly described [13–15]. Relativistic coupled-cluster calculations of NMR shielding constants are simplified for a compound with high space symmetry such as BiF_6^- [5]. Nevertheless, approximations such as using a small contracted basis set and application of restricted kinetic balance to minimize the number of small-component basis functions are necessary to reduce the high computational costs. From the computational point of view, aqueous heavy cation complexes are too large systems with too low space symmetry and, for the final relativistic bismuth shielding, we therefore apply the DKS approach with various modifications of the PBE0 functional.

For bare Bi^{3+} and Bi^{5+} ions, the only contribution to the nonrelativistic NMR shielding is the diamagnetic term, known to be insensitive to the electron correlation. The shielding values differ by less than 1 ppm for various applied nonrelativistic correlation methods (see Table I; for a more detailed discussion of similarly small effects in the case of rare-gas atoms, see Ref. [39]).

The CCSD correlation contribution to $\sigma(^{209}\mathrm{Bi})$ for three symmetrized aqueous complexes and in BiF_6^- is between −400 and −500 ppm and the CCSD(T) value, available only for BiF_6^- and $(Bi(H_2O)_6)^{3+}$, indicates further decrease by about 100 ppm. A ΔCCSD(T) contribution of the same magnitude was obtained using the smaller DZP.dz basis set also for the symmetrized anion containing complexes (see Table I).

We note that the agreement between MP2 and CCSD(T) shielding constants is systematic for the studied complexes.

TABLE I. NMR shielding constants of bismuth in various chemical environments (in ppm).

	Nonrelativistic						Relativistic		
Structure	HF	MP2	CCSD	CCSD(T)	PBE0	PBE0-50[a]	DHF	DKS/PBE0	DKS/PBE0-50
Bi^{3+}	10208	10208	10208	10208	10208	10210	17685	17696	17693
Bi^{5+}	10191	10191	10191	10191	10191	10193	17680	17684	17684
BiF_6^-	7188	6632	6744	6665	6423	6683	14610	12501	13306
$(Bi(H_2O)_6)^{3+}$	8223	7709	7821	7720	7336	7686	14067	11897	12743
$(Bi(H_2O)_5NO_3)^{2+}$	8203	7575	7723	7602[b]	7253	7626	13660	11320	12204
$(Bi(H_2O)_5ClO_4)^{2+}$	8248	7747	7854	7756[b]	7393	7734	13875	11859	12721
$(Bi(H_2O)_6NO_3)^{2+}$	8284	7681			7357	7715	13874	11811	12579
$(Bi(H_2O)_7ClO_4)^{2+}$	8432	7891			7535	7890	14324	11942	12918

[a]Nonrelativistic limit from DKS calculations.
[b]ΔCCSD(T) contribution calculated using the DZP.dz basis set added to the CCSD/uANO.dz value.

Independent of the number of water molecules or the presence of nitrate or perchlorate ion in the solvation shell, for all the discussed aqueous complexes, the bismuth shielding fits into the narrow interval of ≈200 ppm (Table I, Fig. 3), indicating that the nature of intermolecular interactions is the same for all complexes. Therefore, we shall assume that MP2 nonrelativistic shielding values represent a reliable approximation to the CCSD(T) results for the larger bismuth aqueous complexes also.

Considering these findings, the systematic error of the DFT/PBE0 functional for the prediction of bismuth shielding in these complexes can be assessed against higher-quality correlation methods (Table I). The PBE0 functional predicts the correlation contribution to the bismuth shielding to be about −900 ppm, underestimating the coupled-cluster results by about 350 ppm on average.

In the relativistic approach, comparing the DKS/PBE0 and DHF results in Table I, we find that DKS/PBE0 predicts a correlation contribution of about −2000 ppm, twice as large as the nonrelativistic value, and therefore the systematic error of DKS/PBE0 is expected to be proportionally larger.

In summary, the present data indicate (similarly to Ref. [5]) that the DKS/PBE0 method underestimates the bismuth shielding. To reduce this systematic error of DKS/PBE0, we apply three different approximations as follows:

(A) At the nonrelativistic level, we introduce a correction Δ_{PBE0} defined as the difference between correlated results approximated by MP2 and nonrelativistic PBE0 values. To obtain the final value of the shielding, this correction is added to the relativistic DKS/PBE0 shielding constant: $\sigma_A = \sigma(\mathrm{DKS/PBE0}) + \Delta_{\mathrm{PBE0}}$. A similar correction calculated as the difference between relativistic coupled-cluster and DKS/PBE0 values was used in Ref. [5]. For BiF_6^-, our nonrelativistic correction is $\Delta_{\mathrm{PBE0}} = 209$ ppm and the analogous relativistic correction is 437 ppm [5].

(B) In the DKS framework, the amount of HF exchange is increased from 25% in the standard PBE0 functional to 50%. This modified functional (denoted PBE0-50) reproduces nonrelativistic CCSD(T) shielding constants with accuracy better than 50 ppm and this holds for all the investigated chemical environments of bismuth. The nonrelativistic PBE0-50 values were determined from DKS by scaling the speed of light by a factor of 50 (a point model for the nucleus was used in these calculations to compare properly with nonrelativistic counterparts).

We note that modified PBE0 functionals, in particular PBE0-50, have been applied successfully to study NMR parameters at nonrelativistic and relativistic levels (see, e.g., Refs. [40,41] for calculations of shielding constants and [42,43] for the spin-spin coupling constants). We shall use DKS/PBE0-50 values as our best approximation of the bismuth shielding.

(C) The electron correlation contribution Δ_{MP2} calculated in the nonrelativistic approximation as the difference between MP2 and HF results is added to the DHF results: $\sigma_C = \sigma(\mathrm{DHF}) + \Delta_{\mathrm{MP2}}$. In practice, Δ_{MP2} is always negative.

The bismuth shielding constants calculated at the DHF and DKS levels using the uANO.udz basis set are close to the basis-set limit, as illustrated in Table II for DKS/PBE0-50. The quality of the basis set for light elements has a small effect on the shielding of the central bismuth atom. Thus, we assume that the largest contribution to the systematic error of $\sigma(^{209}\mathrm{Bi})$ stems from the uncertainty of the correlation contribution.

TABLE II. Basis-set convergence of ^{209}Bi NMR shielding constants (in ppm), using DKS/PBE0-50 and Dyall's valence double-zeta (vDZ), triple-zeta (vTZ), and quadruple-zeta (vQZ) basis sets. For comparison, results for uANO.udz basis set are included.

	BiF_6^-	$(Bi(H_2O)_6NO_3)^{2+}$	$(Bi(H_2O)_7ClO_4)^{2+}$
Dyall vDZ	13266	12472	12819
Dyall vTZ	13316	12565	12911
Dyall vQZ	13334	12589	12940
uANO.udz	13306	12579	12918

We find that for these approximations, the following inequality holds: $\sigma_A < \sigma_B < \sigma_C$. The approximations (A) and (C) provide estimates of the lower and upper limit of the bismuth shielding, respectively. Therefore, we have estimated asymmetric error bars for the bismuth shielding as $\sigma_B - \sigma_A$ and $\sigma_C - \sigma_B$. The final NMR shielding constants in aqueous complexes and BiF_6^- with the asymmetric error bars evaluated using the (A), (B), and (C) approximations are collected in Table III and are used to derive the magnetic moment of ^{209}Bi.

IV. NUCLEAR MAGNETIC DIPOLE MOMENTS

The magnetic moment of ^{209}Bi is derived from the equation

$$\mu_I(^{209}\mathrm{Bi}) = 9\,\frac{\nu(^{209}\mathrm{Bi})}{\nu(^{1}\mathrm{H})}\,\frac{1-\sigma(^{1}\mathrm{H})}{1-\sigma(^{209}\mathrm{Bi})}\,\mu_I(^{1}\mathrm{H}), \qquad (1)$$

where we use the experimental frequency ratio $\nu(^{209}\mathrm{Bi})/\nu(^{1}\mathrm{H})$, the reference shielding of ^{1}H in TMS $\sigma(^{1}\mathrm{H}) = 33.480$ ppm [44], $\sigma(^{209}\mathrm{Bi})$ of different bismuth complexes, and the reference proton magnetic moment $\mu_I(^{1}\mathrm{H}) = 2.792\,847\,356(23)\ \mu_N$ [45]. The factor of 9 represents the ratio of nuclear spins.

The final values for the nuclear magnetic moments are collected in Table III and are depicted in Fig. 4 together with $\mu_I(^{209}\mathrm{Bi})$ from the NMR experiment and the specific

TABLE III. Comparison of the ^{209}Bi nuclear magnetic dipole moments (in μ_N) from various experiments.

Sample	Frequency ratio[a]	$\sigma(^{209}\mathrm{Bi})$	$\mu_I(^{209}\mathrm{Bi})$	Source
$Bi(NO_3)_3$	0.160702(1)	12579^{+692}_{-444}	$4.0907(^{+28}_{-19})$	This work
$Bi(ClO_4)_3$	0.160697(1)	12918^{+865}_{-620}	$4.0919(^{+36}_{-25})$	This work
BiF_6^-	0.1607167(2)[b]	13306^{+781}_{-563}	$4.0941(^{+32}_{-24})$	This work
	0.1607167(2)	12792	4.092(2)	Ref. [5]
			4.0900(15)	From HFS
				Ref. [5]
			4.1106(2)[c]	NMR

[a]Bismuth NMR frequency ratio with respect to ^{1}H in liquid TMS.
[b]See Ref. [5].
[c]The presently used literature value [1] is based on the 1953 data of Ref. [46].

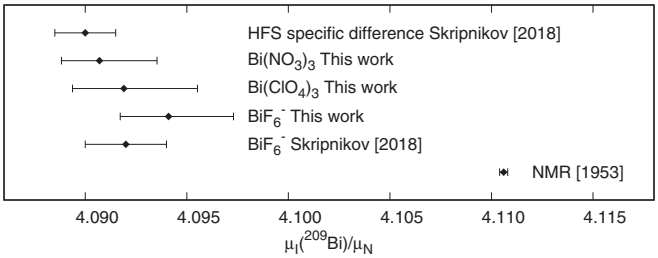

FIG. 4. Magnetic dipole moment of ^{209}Bi from different sources. "Skripnikov [2018]" represents Ref. [5]. "BiF_6^- This work" is based on the experiment of Ref. [5] and our shielding calculations. The "NMR [1953]" value is from Refs. [1,46].

difference by Skripnikov *et al.* and the old literature value from NMR experiment [1,46]. Our values of ^{209}Bi magnetic moment correspond to the use of σ_B, i.e., approximation (B) to $\sigma(^{209}\mathrm{Bi})$. In the asymmetric error-bar definition, the left-hand error-bar termination represents the magnetic moment derived using σ_A and the right-hand error bar is derived using σ_C. Our $\mu_I(^{209}\mathrm{Bi})$ values predicted from $Bi(NO_3)_3$ and $Bi(ClO_4)_3$ experiment and calculations are consistent, differing only by 0.001 μ_N, and they are also both consistent with the value 4.092(2) μ_N obtained by Skripnikov. Using the same approximation (B) for $\sigma(^{209}\mathrm{Bi})$ in BiF_6^-, we obtain, for the nuclear magnetic moment, 4.0941 μ_N, which lies at the borderline of the result of Skripnikov *et al.* [5]

V. CONCLUSIONS

Our values for the ^{209}Bi magnetic moment are based, similarly to that of Skripnikov *et al.* [5], on the DKS approximation, which is a practical and computationally feasible method applicable to the shielding calculations of bismuth complexes. Comparison with the coupled-cluster results indicates that the PBE0 functional underestimates the total shielding due to inaccurate description of the relevant electron correlation effects. We have corrected this systematic error applying the PBE0-50 functional with 50% of HF exchange-term content. The calculations of our aqueous Bi^{3+} complexes, which model the experiment properly taking into account the main solvent effects, yield magnetic moment values much closer to the recent value of the ^{209}Bi magnetic moment obtained by Skripnikov *et al.* [5] than the old literature NMR-based value. Moreover, with the DKS/PBE0-50 approximation, regardless of the model complex (aqueous Bi^{3+} or BiF_6^-), all rederived ^{209}Bi magnetic moment values are contained in a narrow interval of $3 \times 10^{-3}\mu_N$, with large overlap of the error bars with the ^{209}Bi magnetic moment given in Ref. [5]. Our magnetic moment values determined studying aqueous complexes were obtained using different theoretical approaches for the bismuth shielding and different NMR experiments than those of Skripnikov *et al.*, and thus the present results provide an independent confirmation of the recent value of the magnetic dipole moment of ^{209}Bi.

ACKNOWLEDGMENTS

We acknowledge financial support from Slovak Grants No. APVV-15-0105 and No. VEGA 1/0279/16. Computational resources were provided by The Norwegian Supercomputing program NOTUR (Grant No. NN4654K), HPC Cluster of Slovak University of Technology and Computing Center of the Slovak Academy of Sciences (Projects ITMS No. 26230120002 and No. 26210120002), and IT4Innovations National Supercomputing Center - Grant No. LM2015070 (The Ministry of Education, Youth and Sports of The Czech Republic from the Large Infrastructures for Research, Experimental Development and Innovations, Project No. IF OPEN-12-40). Funding by the ERDF - Research and Development Operational Programme under the project "University Scientific Park Campus MTF STU - CAMBO" Project ITMS No. 26220220179 is also acknowledged. We are indebted to Kenneth Ruud for reading and commenting on the manuscript.

APPENDIX A: SAMPLES PREPARATION

Solid bismuth(III) perchlorate [$Bi(ClO_4)_3$] is a shock-sensitive explosive [47] and not available as a pure chemical compound. However, its aqueous solutions can be prepared from solid bismuth(III) chloride ($BiCl_3$), perchloric acid ($HClO_4$), and silver perchlorate ($AgClO_4$). In our experiment, the low solubility of silver chloride (AgCl) was utilized for the elimination of chloride anions (Cl^-) from the aqueous solutions containing bismuth cations (Bi^{3+}) and perchlorate anions (ClO_4^-). Samples of aqueous solutions of bismuth perchlorate were prepared as follows: first, the basic solution containing 1 M $HClO_4$ and 1 M $AgClO_4$ in triply distilled water was step-by-step mixed with small amounts of anhydrous powdered $BiCl_3$ until the precipitation of AgCl was quantitatively completed and solid AgCl was immediately removed. Next, the basic solution was used for the preparation of samples containing various concentrations of Bi^{3+} cations after the dilution with pure water. Preparation of $Bi(NO_3)_3$ aqueous solution was straightforward. Weighted amounts of pure bismuth nitrate pentahydrate [$Bi(NO_3)_3{\cdot}5H_2O$] were directly dissolved in 10% aqueous solution of nitric acid (HNO_3). All the ^{209}Bi NMR measurements of the above samples were performed immediately after solution preparation to avoid degradation processes in solutions. All the above chemical compounds were of high purity (>99.99%) and supplied by Sigma-Aldrich, Inc.

APPENDIX B: BISMUTH COMPLEXES—STRUCTURE OPTIMIZATION

The structures of the aqueous solvation shell of Bi^{3+} with a perchlorate or nitrate anion were optimized at the density functional theory (DFT) level to model the conditions in aqueous $Bi(ClO_4)_3$ and $Bi(NO_3)_3$ solutions, respectively. To this end, two different models were used: (a) DFT using the B3LYP functional [48] corrected by Grimme's D3 dispersion term [49], and (b) DFT with B3LYP and D3 dispersion correction and the implicit solvent model COSMO [50] for modeling of solvent effects of higher solvation shells. The dielectric constant of 78 for water was used in the COSMO model. We have used the Def2-TZVP basis set for Bi [51] with a core potential describing 60 core electrons, and the DZP basis set [52] for H, N, O, and Cl atoms. The structures were optimized using the NWChem package [33].

TABLE IV. Average distances in the solvation shell of Bi^{3+}.

Structure	Distance	Solvent model[a] A	B	Expt.
$(Bi(H_2O)_7ClO_4)^{2+}$	Bi-O	2.56	2.45	2.411(5)[b]
	Bi-Cl	3.07	3.76	3.76(4)[b]
$(Bi(H_2O)_6NO_3)^{2+}$	Bi-O	2.49	2.49	
	Bi-N	2.76	2.95	

[a]Solvent model A: the first solvation shell modeled explicitly at the DFT+D3 level. Solvent model B: the first solvation shell modeled explicitly at the DFT+D3 level with COSMO solvent model for higher shells.
[b]Reference [26].

The initial structures of Bi^{3+} with perchlorate anion were prepared as follows: seven water molecules and one perchlorate anion were placed in the vertices of a cube or square antiprism, keeping Bi^{3+} in the center. Bi-O axial rotational randomness was introduced for all coordinated species to obtain a set of different initial structures of $(Bi(H_2O)_7ClO_4)^{2+}$. In the case of the Bi^{3+} aqueous solvation shell with nitrate anion, optimization showed that the coordination structure of one nitrate anion with six water molecules is preferred. An additional water molecule escaped to the second solvation shell during the optimization. Coordination of two oxygen atoms of NO_3^- to Bi^{3+} was energetically favorable. This structure preserves a Bi-O coordination of eight as also found for the perchlorate solution. Taking into account these findings, the initial $(Bi(H_2O)_6NO_3)^{2+}$ structures were modeled by placing six water molecules and a nitrate anion randomly to the vertices of a pentagonal bipyramid surrounding a central Bi^{3+} cation, keeping eightfold Bi-O coordination. Axial rotational randomness of coordinated species was used to prepare a set of different initial structures. For all initial perchlorate and nitrate structures the initial Bi-O distances of 2.5 Å were used.

The energy-optimization procedure yields about 30 distinct structures of $(Bi(H_2O)_7ClO_4)^{2+}$ and $(Bi(H_2O)_6NO_3)^{2+}$ complexes representing different local minima on the potential-energy hypersurface. In both data sets, the complexes with the lowest energies were identified and next used as model solvation structures for the following NMR shielding calculations. These optimal structures are depicted in Figs. 2(a) and 2(b). The relevant average internuclear distances in these two structures are collected in Table IV. The implicit solvent model COSMO was found to be crucial to reach good agreement with the experimental structural data of the $(Bi(H_2O)_7ClO_4)^{2+}$ complex.

Three artificial bismuth solvation shell structures with higher space symmetry were optimized using the same method: $(Bi(H_2O)_5NO_3)^{2+}$ and $(Bi(H_2O)_5ClO_4)^{2+}$ with C_{2v} symmetry point group [Figs. 2(c) and 2(d)] and $(Bi(H_2O)_6)^{3+}$ with D_{2h} symmetry point group.

The structure of BiF_6^- was optimized using the B3LYP functional with D3 correction and COSMO implicit solvent model with dielectric constant corresponding to acetonitrile solvent. Def2-TZVP with 60 electron core potential and the TZVP basis set were used for bismuth and fluorine atoms, respectively. The optimal Bi-F interatomic distance was found to be 2.0172 Å.

[1] N. J. Stone, At. Data Nucl. Data Tables **90**, 75 (2005).
[2] I. Klaft, S. Borneis, T. Engel, B. Fricke, R. Grieser, G. Huber, T. Kühl, D. Marx, R. Neumann, S. Schröder, P. Seelig, and L. Völker, Phys. Rev. Lett. **73**, 2425 (1994).
[3] J. Ullmann, Z. Andelkovic, C. Brandau, A. Dax, W. Geithner, C. Geppert, C. Gorges, M. Hammen, V. Hannen, S. Kaufmann, K. König, Y. A. Litvinov, M. Lochmann, B. Maaß, J. Meisner, T. Murböck, R. Sánchez, M. Schmidt, S. Schmidt, M. Steck, T. Stöhlker, R. C. Thompson, C. Trageser, J. Vollbrecht, C. Weinheimer, and W. Nörtershäuser, Nat. Commun. **8**, 15484 (2017).
[4] J.-P. Karr, Nat. Phys. **13**, 533 (2017).
[5] L. V. Skripnikov, S. Schmidt, J. Ullmann, C. Geppert, F. Kraus, B. Kresse, W. Nörtershäuser, A. F. Privalov, B. Scheibe, V. M. Shabaev, M. Vogel, and A. V. Volotka, Phys. Rev. Lett. **120**, 093001 (2018).
[6] M. G. H. Gustavsson and A. M. Mårtensson-Pendrill, Phys. Rev. A **58**, 3611 (1998).
[7] A. Antušek, K. Jackowski, M. Jaszuński, W. Makulski, and M. Wilczek, Chem. Phys. Lett. **411**, 111 (2005).
[8] J. Gauss, Chem. Phys. Lett. **191**, 614 (1992).
[9] J. D. Watts, J. Gauss, and R. J. Bartlett, J. Chem. Phys. **98**, 8718 (1993).
[10] J. Gauss and J. F. Stanton, J. Chem. Phys. **102**, 251 (1995).
[11] T. Helgaker, M. Jaszuński, and K. Ruud, Chem. Rev. **99**, 293 (1999).
[12] M. Bühl, M. Kaupp, O. L. Malkina, and V. G. Malkin, J. Comput. Chem. **20**, 91 (1999).
[13] *Calculation of NMR and EPR Parameters. Theory and Applications*, edited by M. Kaupp, M. Bühl, and V. G. Malkin (Wiley–VCH, Weinheim, 2004).
[14] M. Reiher and A. Wolf, *Relativistic Quantum Chemistry* (Wiley-VCH, Weinheim, 2009).
[15] M. Repisky, S. Komorovsky, R. Bast, and K. Ruud, in *Gas Phase NMR*, edited by K. Jackowski and M. Jaszuński (The Royal Society of Chemistry, Cambridge, 2016), Chap. 8, pp. 267–303.
[16] M. Jaszuński and K. Jackowski, in *Lecture Notes in Physics*, Vol. 745, edited by S. G. Karshenboim (Springer, Berlin, 2008), pp. 233–260.
[17] M. Jaszuński, A. Antušek, P. Garbacz, K. Jackowski, W. Makulski, and M. Wilczek, Progr. Nucl. Magn. Reson. Spectrosc. **67**, 49 (2012).
[18] *Gas-phase NMR*, edited by K. Jackowski and M. Jaszuński (The Royal Society of Chemistry, Cambridge, 2016).
[19] A. Antušek, D. Kędziera, A. Kaczmarek-Kędziera, and M. Jaszuński, Chem. Phys. Lett. **532**, 1 (2012).
[20] A. Antušek, P. Rodziewicz, D. Kędziera, A. Kaczmarek-Kędziera, and M. Jaszuński, Chem. Phys. Lett. **588**, 57 (2013).
[21] A. Antušek and F. Holka, J. Chem. Phys. **143**, 074301 (2015).
[22] A. Antušek and M. Šulka, Chem. Phys. Lett. **660**, 127 (2016).

[23] B. Adrjan, W. Makulski, K. Jackowski, T. B. Demissie, K. Ruud, A. Antušek, and M. Jaszuński, Phys. Chem. Chem. Phys. **18**, 16483 (2016).
[24] R. Ayala, J. M. Martínez, R. R. Pappalardo, and E. S. Marcos, J. Phys. Chem. B **116**, 14903 (2012).
[25] J. Brugger, B. Tooth, B. Etschmann, W. Liu, D. Testemale, J.-L. Hazemann, and P. V. Grundler, J. Solution Chem. **43**, 314 (2014).
[26] J. Näslund, I. Persson, and M. Sandström, Inorg. Chem. **39**, 4012 (2000).
[27] J. P. Perdew, M. Ernzerhof, and K. Burke, J. Chem. Phys. **105**, 9982 (1996).
[28] C. Adamo and V. Barone, J. Chem. Phys. **110**, 6158 (1999).
[29] B. O. Roos, R. Lindh, P.-Å. Malmqvist, V. Veryazov, and P.-O. Widmark, J. Phys. Chem. A **108**, 2851 (2004).
[30] T. H. Dunning Jr., J. Chem. Phys. **90**, 1007 (1989).
[31] K. Wolinski, J. F. Hinton, and P. Pulay, J. Am. Chem. Soc. **112**, 8251 (1990).
[32] J. F. Stanton, J. Gauss, M. E. Harding, and P. G. Szalay, with contributions from A. A. Auer, R. J. Bartlett, U. Benedikt, C. Berger, D. E. Bernholdt, J. Bomble, L. Cheng, O. Christiansen, M. Heckert, O. Heun, C. Huber, T.-C. Jagau, D. Jonsson, J. Jusélius, K. Klein, W. J. Lauderdale, D. A. Matthews, T. Metzroth, L. A. Mück, D. P. O'Neill, D. R. Price, E. Prochnow, C. Puzzarini, K. Ruud, F. Schiffmann, W. Schwalbach, C. Simmons, S. Stopkowicz, A. Tajti, J. Vázquez, F. Wang, and J. D. Watts, computer code CFOUR, a quantum chemical program package. Also, the integral packages by J. Almlöf and P. R. Taylor, computer code MOLECULE; P. R. Taylor, computer code PROPS; and T. Helgaker, H. J. Aa. Jensen, P. Jørgensen, and J. Olsen, computer code ABACUS; as well as ECP routines by A. V. Mitin and C. van Wüllen. For the current version, see http://www.cfour.de (unpublished).
[33] M. Valiev, E. J. Bylaska, N. Govind, K. Kowalski, T. P. Straatsma, H. J. J. van Dam, D. Wang, J. Nieplocha, E. Apra, T. L. Windus, and W. de Jong, Comput. Phys. Commun. **181**, 1477 (2010).
[34] K. G. Dyall, Theor. Chem. Acc. **115**, 441 (2006).
[35] S. Komorovský, M. Repiský, O. L. Malkina, V. G. Malkin, I. M. Ondík, and M. Kaupp, J. Chem. Phys. **128**, 104101 (2008).
[36] S. Komorovský, M. Repiský, O. L. Malkina, and V. G. Malkin, J. Chem. Phys. **132**, 154101 (2010).
[37] L. Visscher and K. G. Dyall, At. Data Nucl. Data Tables **67**, 207 (1997).
[38] M. Repisky, S. Komorovsky, V. G. Malkin, O. L. Malkina, M. Kaupp, and K. Ruud, with contributions from R. Bast, R. Di Remigio, U. Ekstrom, M. Kadek, S. Knecht, L. Konecny, E. Malkin, and I. Malkin Ondik, computer code ReSpect 5.0.1 (2018), a relativistic spectroscopy DFT program; http://www.respectprogram.org (unpublished).
[39] J. Vaara and P. Pyykkö, J. Chem. Phys. **118**, 2973 (2003).
[40] F. Alkan, S. T. Holmes, and C. Dybowski, J. Chem. Theory Comp. **13**, 4741 (2017).
[41] P. Hrobárik, V. Hrobáriková, A. H. Greif, and M. Kaupp, Angew. Chem. Int. Ed. Engl. **51**, 10884 (2012).
[42] D. L. Bryce and J. Autschbach, Can. J. Chem. **87**, 927 (2009).
[43] M. Jaszuński, A. Antušek, T. B. Demissie, S. Komorovsky, M. Repisky, and K. Ruud, J. Chem. Phys. **145**, 244308 (2016).
[44] P. Garbacz, K. Jackowski, W. Makulski, and R. E. Wasylishen, J. Phys. Chem. **A 116**, 11896 (2012).
[45] P. J. Mohr, B. N. Taylor, and D. B. Newell, Rev. Mod. Phys. **80**, 633 (2008).
[46] Y. Ting and D. Williams, Phys. Rev. **89**, 595 (1953).
[47] D. G. Nicholson and J. H. Reedy, J. Am. Chem. Soc. **57**, 817 (1935).
[48] A. D. Becke, J. Chem. Phys. **98**, 5648 (1993).
[49] S. Grimme, J. Antony, S. Ehrlich, and H. Krieg, J. Chem. Phys. **132**, 154104 (2010).
[50] A. Klamt and G. Schüürmann, J. Chem. Soc., Perkin Trans. 2, 799 (1993).
[51] F. Weigend and R. Ahlrichs, Phys. Chem. Chem. Phys. **7**, 3297 (2005).
[52] A. C. Neto, E. Muniz, R. Centoducatte, and F. Jorge, J. Mol. Struct. THEOCHEM **718**, 219 (2005).